

# Efficient Amplification of Photonic Qubits by Optimal Quantum Cloning

Karol Bartkiewicz,<sup>1,2,\*</sup> Antonín Černoš,<sup>2</sup> Karel Lemr,<sup>2</sup> Jan Soubusta,<sup>3</sup> and Magdalena Stobińska<sup>4,5</sup>

<sup>1</sup>*Faculty of Physics, Adam Mickiewicz University, PL-61-614 Poznań, Poland*

<sup>2</sup>*RCPTM, Joint Laboratory of Optics of Palacký University and  
Institute of Physics of Academy of Sciences of the Czech Republic,  
17. listopadu 12, 772 07 Olomouc, Czech Republic*

<sup>3</sup>*Institute of Physics of Academy of Science of the Czech Republic,  
Joint Laboratory of Optics of PU and IP AS CR,  
17. listopadu 50A, 77207 Olomouc, Czech Republic*

<sup>4</sup>*Institute of Theoretical Physics and Astrophysics,  
University of Gdańsk, ul. Wita Stwosza 57, 80-952 Gdańsk, Poland*

<sup>5</sup>*Institute of Physics, Polish Academy of Sciences, Al. Lotników 32/46, 02-668 Warsaw, Poland*

We demonstrate that a phase-independent quantum amplifier of a polarization qubit is a complementary amplifier of the heralded qubit amplifier [N. Gisin, S. Pironio and N. Sangouard, Phys. Rev. Lett. **105**, 070501 (2010)]. It employs the multi-functional cloner in  $1 \rightarrow 2$  copying regime, capable of providing approximate copies of qubits given by various probability distributions, and is optimized for distributions with axial symmetry. Direct applications of the proposed solution are possible in quantum technologies, doubling the range where quantum information is coherently broadcast. It also outperforms natural nonlinear amplifiers that use stimulated emission in bulk nonlinear materials. We consider the amplifier to be an important tool for amplifying quantum information sent via quantum channels with phase-independent damping.

PACS numbers: 03.67.Mn, 03.65.Ud, 42.50.Dv

## I. INTRODUCTION

Photons are the best long-distance information carriers, although transmission channels are inevitably lossy. However, overcoming the problem of transmission loss for long-distance quantum communication is a challenging problem which seems not to have an apparent solution. This seriously limits the development of quantum technologies.

There have been several proposals on how to increase the efficiency of quantum information transfer including quantum repeaters (employing entanglement swapping [1] or quantum cloning [2]) and heralded qubit amplifiers [3]. A qubit is the smallest amount of quantum information represented by a vector in two dimensional Hilbert space. Its natural optical implementation is the polarization of a single photon represented on the Poincaré sphere in Fig. 1 (left). Solving the problem of extending the range of quantum optical signals is essential for photonic quantum technologies: quantum communication, cryptography and metrology. Cloners and amplifiers are useful not only for improving the effectiveness of quantum communication, they are also promising means of closing the detection loophole, paving the way to irrefutable Bell tests [4, 5] and device-independent QKD [3].

Recently, a heralded noiseless amplifier of polarization qubits has been proposed and [3] and implemented [6]. The heralded amplifier and its improvements (see, eg., Ref. [7]) or alternative schemes using entanglement [8–10] have been demonstrated to be useful especially in the

context of quantum key distribution. Interestingly the improved qubit amplifier described in Ref. [8] is closely related to entanglement swapping, which suggests that there is a strong connection between qubit amplifiers and quantum repeaters (or relays), which are both based on similar underlying ideas. The heralded amplifier announces the time of arrival of optical signals. By doing so it increases the probability of receiving the signal after it was announced. This means that we are only waiting for a photon once it has been announced. Thus, this approach could spare us some time otherwise wasted on waiting for the unannounced signal. The amplifier works with an arbitrary gain (increase in of the probability of registering a photon) without introducing noise, but the probability of successfully heralding event decreases as the gain is increased. In the case of the original proposal, perfect gain could have been reached only asymptotically, however this shortcoming has been removed by Pitkanen *et al.* [7]. Recently, it has been shown that, if a heralded amplifier is allowed to introduce some noise, its gain and heralding rate can be increased [10] which also depends on the set of qubits to be amplified.

Instead of increasing the probability of receiving the signal by announcing its expected arrival one can use an alternative strategy based on sending multiple copies of the signal through the lossy channel. This means that we will receive a message faster, because there is no reason for repeating it once it was sufficiently amplified. Similarly as before this approach can save us some time. There is however, a fundamental problem with this approach when we try to apply it in case of single photons in unknown quantum states. In classical world the weak signal is analyzed and then a stronger version of

\* bark@amu.edu.pl

it is produced and send further. This allows us to make the signal arbitrarily strong which makes it more robust against transmission losses. However, in quantum regime measuring the signal in a wrong basis will introduce errors. Moreover, according to the no-cloning theorem [11], quantum information cannot be perfectly copied or amplified.

The best copying results are achieved by optimal quantum cloning machines (QCMs) [12, 13]. They are crucial for analyzing the security of quantum key distribution (QKD) against coherent and incoherent attacks [14, 15], and limit the capacity of quantum channels [16]. They provide the highest fidelity  $\mathcal{F}$  between the original qubit and its copies, see Fig. 1(right). Universal QCMs operate equally well for all qubits, with  $\mathcal{F} = 5/6$  for two copies ( $1 \rightarrow 2$ ) [12]. State-dependent cloners can exceed this fidelity for some subspaces of the sphere [13] using partial information about the input qubit distribution. Examples include the phase-covariant cloner [13, 17] optimal for equatorial states; and its generalizations to phase-independent cloners [18–23], optimal for qubits with axially-symmetric distributions, e.g., Fisher [24], Brosseau [25], and Henyey-Greenstein [26] distributions. These distributions are used to describe many problems of directional statistics [27] in physics, astronomy, biology, geology and psychology.

Can we construct a useful qubit amplifier that will make use of the classical repetition scheme by using the best approximate quantum cloning operations? To answer this question let us consider an erasure channel. If we replace each of the deleted qubits with a random state, we deal with a depolarizing channel. According to HSW (Holevo-Schumacher-Westmoreland) theorem [28], depolarizing channel  $\mathcal{E} : \rho \rightarrow \eta\rho + (1-\eta)\mathbb{1}/2$ , where  $\rho$  is a pure state, yields product state capacity of

$$C(\mathcal{E}) = 1 - H\left(\frac{1+\eta}{2}\right), \quad (1)$$

where  $H(x) = -x\log_2 x - (1-x)\log_2(1-x)$  is binary entropy. If we prepare two clones of the pure input state  $\rho$  with fidelity  $F$  and then send them both through the channel, the effective transformation (for small  $\eta$ ) turns out to be  $\mathcal{E}' : \rho \rightarrow \eta'\rho + (1-\eta')\mathbb{1}/2$ , where  $\eta' = 2(2F-1)\eta$  (for details see Sec. II). If  $4F-2 > 1$ , we can increase product state capacity by applying quantum cloning. In particular, this is true for universal cloning [12], where  $F = 5/6$ , but not for classical cloning for which  $F = 3/4$ . Therefore, we expect that information can be transmitted more efficiently if amplified by a quantum copying machine which provides fidelity  $F > 3/4$ , i.e.,  $C(\mathcal{E}') > C(\mathcal{E})$ . This holds under assumption that the cloning operation is deterministic or its success probability is sufficiently large, i.e.,  $P > 1/(4F-2)$ . Note, that there is no reason for the cloning process to work with  $P < 1$  other than the implementation-dependent technical issues. However, if we limit ourselves to the framework of linear optics, can such amplifier perform better, in terms of gain or qubit fidelity, than other types of qubit ampli-

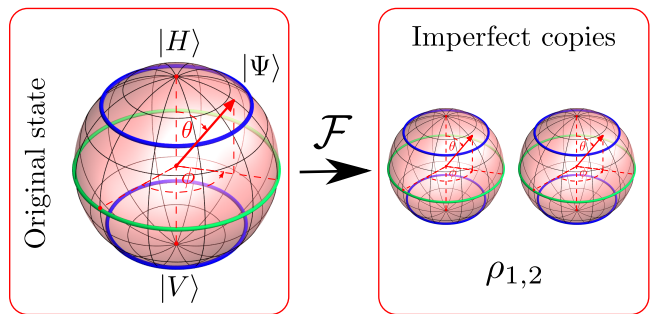


FIG. 1. (Color online) Left: Poincaré sphere of polarization. A qubit is a linear combination of horizontal  $|H\rangle$  (the north pole) and vertical  $|V\rangle$  (the south pole) polarizations:  $|\Psi\rangle = \cos(\theta/2)|H\rangle + e^{i\phi}\sin(\theta/2)|V\rangle$ . Radius of the sphere is 1. The uniform probability distribution of polarization qubit is marked in red. Exemplary distributions with axial symmetry are in green and blue. Right: imperfect copies  $\rho'$  of  $\rho = |\Psi\rangle\langle\Psi|$ .

fiers?

We expect that cloning-based amplifier (CBA) will be directly applicable to quantum technologies by increasing the range over which quantum information is coherently broadcast. It will also outperform natural nonlinear amplifiers that use stimulated emission from bulk nonlinear materials. In this paper we will study cloning-based amplifiers and compare them with heralded amplifiers in terms of qubit fidelity and gain in probability of receiving the amplified signal for various communication scenarios (see Fig. 2). We will demonstrate that in some cases a cloning-based phase-independent quantum amplifier of a polarization qubit outperforms the heralded qubit amplifier [3] (HA) in terms of the provided gain. However, as we show, the CBA performs worse than HA if used at the end of the transmission line. Thus, we conclude that the two types of amplifiers perform complementary tasks. The CBA employs the  $1 \rightarrow 2$  multi-functional cloner [22, 23] optimized for distributions with axial symmetry.

Some universal and phase-covariant QCMs are built using parametric amplifiers and can generate macroscopic quantum states of light [29]. Other implementations use two-photon interference on a polarization sensitive beam splitter [23]. Here we will use the latter approach to experimentally demonstrate a principle of operation of a CBA.

## II. CLONING BASED AMPLIFIER

The CBA preamplifies a qubit through duplication before sending its two copies via a lossy channel (see Fig. 3). One has to feed it with both the amplified qubit and an ancillary qubit. The total probability of finding at least one photon at the output of the CBA working with efficiency  $P = 1$  is  $P_{n>0}^{(\text{CBA})} = 1 - (1-\eta)^2 = (2-\eta)\eta$  (see

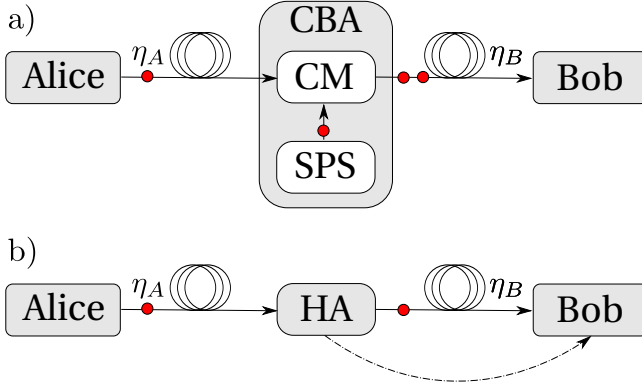


FIG. 2. (Color online) Both cloning-based amplifier (a) and heralded amplifier can be placed in the communication channel of total transmissivity  $\eta = \eta_A \eta_B$  to fight the losses. We assume that Alice sends a photon to Bob who wants to receive the quantum message with minimum time spent on waiting. Because of the channel losses only a fraction of photons will reach Bob. If one uses a qubit amplifier, probability of Bob receiving the signal is increased. In case of the CBA this probability is increased by sending an additional photon generated by a single photon source (SPS). If the HA is used, the probability is increased, by informing Bob when he should be ready to receive a photon so that he does not waste time on waiting in vain.

Fig. 3) which is greater than the analogous probability for a bare channel, where  $P_{n>0}^{(0)} = \eta$ . Assume a photon reaches its destination with probability  $\eta$ . If two photons are sent, the probability that at least one of them arrives is  $2\eta(1 - \eta) + \eta^2$ , i.e., transmission efficiency increases. If the CBA works with efficiency  $P \leq 1$  we have  $P_{n>0}^{(\text{CBA})} = P(2 - \eta)\eta$ . Let us define transmission gain for the CBA as

$$G_T^{(\text{CBA})}(\eta, P) = P \frac{P_{n>0}^{(\text{CBA})}}{P_{n>0}^{(0)}} = (2 - \eta)P. \quad (2)$$

In contrast to HA, the CBA provides gain limited by the number of copies. The device provides a higher gain if  $1 \rightarrow N_{\text{copy}}$  cloning [18, 30] is applied, although the clones have lower fidelity. There are no laws of physics preventing to reach  $P = 1$ , however, this value depends on the particular platform of implementing the amplifier. In the following sections we will focus on the case of  $\eta \ll 1$ , where  $G_T^{(\text{CBA})}(P) = 2P \equiv G$ .

The efficiency  $P$  can be understood as the success probability  $P$  of a copying process  $\rho \rightarrow \rho'$  providing two copies  $\rho'$  of the original qubit  $\rho = |\Psi\rangle\langle\Psi|$  for  $|\Psi\rangle = \cos(\theta/2)|H\rangle + e^{i\phi}\sin(\theta/2)|V\rangle$  with fidelity  $\mathcal{F}$ , so that  $\rho' = (2\mathcal{F} - 1)\rho + (1 - \mathcal{F})\mathbb{1}$  and  $\mathbb{1}/2$  is a maximally mixed state. The intrinsic noise of this operation quantified by inverted signal to noise ratio ( $SNR$ ) decreases along with increasing fidelity  $\mathcal{F}$ . The relation between the  $SNR$  and fidelity is:

$$SNR(\mathcal{F}) = \frac{x}{1-x}, \quad (3)$$

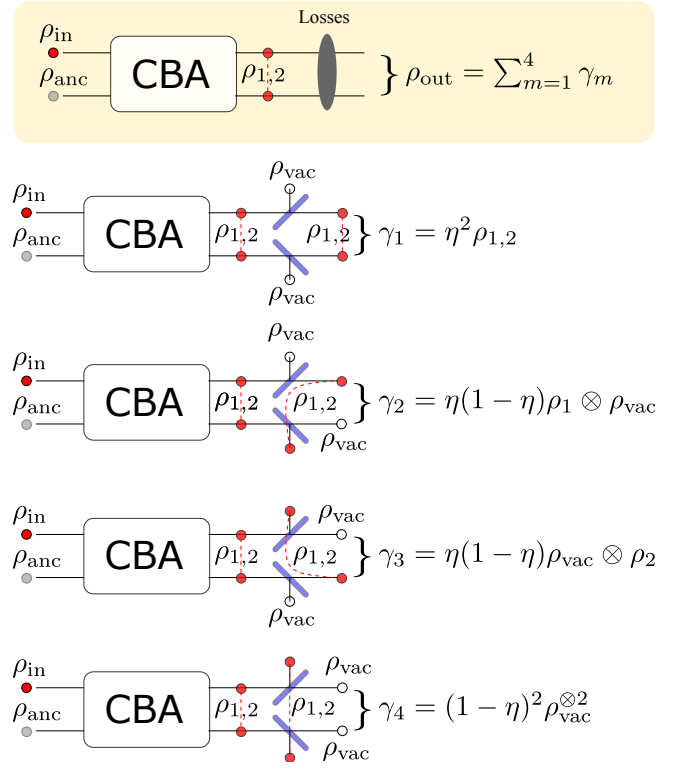


FIG. 3. (Color online) Principle of operation of the CBA working at maximum efficiency  $P = 1$ . The CBA has two input modes for signal qubit  $\rho_{in}$  and ancillary qubit  $\rho_{anc}$ . The output of the CBA is described by state  $\rho_{1,2}$ . The reduced density matrices  $\rho_1 = \text{Tr}_2 \rho_{1,2} = \rho'$  and  $\rho_2 = \text{Tr}_1 \rho_{1,2} = \rho'$  describe each of the two copies of  $\rho_{in} = \rho$  separately. Here we demonstrate how the output state of the amplifier is calculated by modeling losses as beam splitter transformations.

where  $x = 2\mathcal{F} - 1$ . In perfect copying  $\mathcal{F} = 1$  and the  $SNR \rightarrow \infty$ . For the best classical cloning of an unknown qubit  $SNR = 1$  (0 dB) for  $\mathcal{F} = 0.75$ . Thus, we will use this  $SNR$  value as a threshold for quantum amplification. Figure 4 depicts the  $SNR$  as a function of gain and specific qubit distributions. Now, we can express the condition on increasing product state capacity for depolarizing channel defined in Eq. (1) as

$$G > 1 + SNR^{-1}, \quad (4)$$

where  $G = 2P$ , i.e., for  $\eta \ll 1$ .

#### A. Applying hybrid quantum-classical cloning

As we know from the previous section, for small values of  $\eta \ll 1$  the gain of the CBA reads  $G \equiv G_T^{(\text{CBA})} = 2P$ , where  $P$  can be arbitrarily close to 1. However, in linear optical quantum cloning experiments the value of  $P$  is lower. The CBA performs optimal amplification of qubits whose distribution on the Bloch sphere is axially symmetric. The quantum cloning strategy in [22] is optimal for

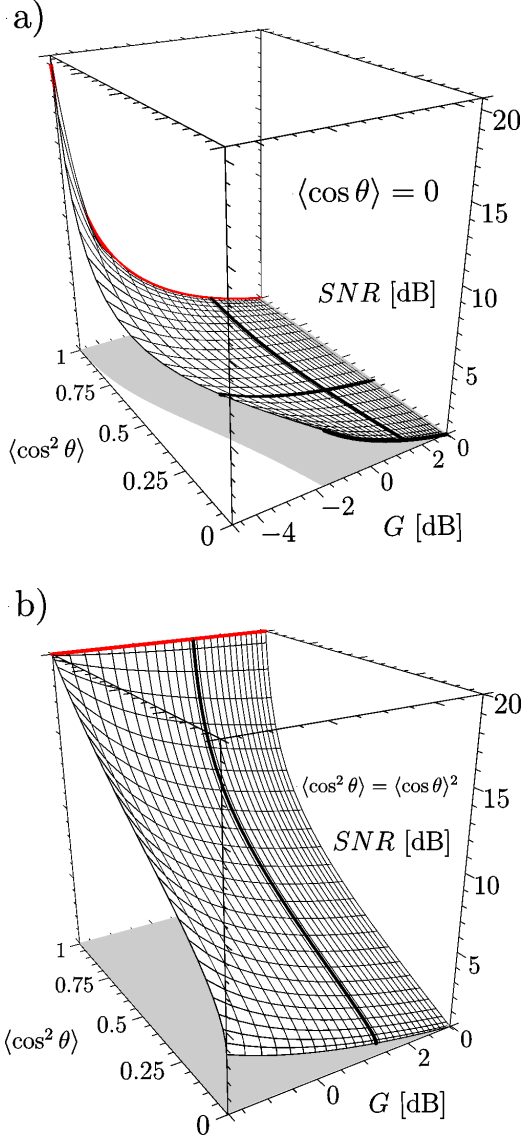


FIG. 4. (Color online) Signal to noise ratio  $SNR$  versus gain  $G$  for a given input qubit distribution quantified by  $\langle \cos^n \theta \rangle$  for  $n = 1, 2$  fully characterizes the CBA. (a): we assumed distributions with  $\langle \cos \theta \rangle = 0$ ; if  $\langle \cos^2 \theta \rangle = 1/3$ , the amplifier is universal; if  $\langle \cos^2 \theta \rangle = 0$  the amplifier is phase-covariant optimized for equatorial qubits. If  $\langle \cos^2 \theta \rangle = 1$  (red curve) then the signal can be amplified classically with infinite  $SNR$  ratio because the states of  $\cos \theta = \pm 1$  can be discriminated deterministically. (b): if the state of the qubit is known *a priori*, e.g.  $\cos \theta = \pm 1$ ,  $\langle \cos^2 \theta \rangle = \langle \cos \theta \rangle^2$ , the qubit can be amplified with an arbitrarily high gain (red curve). Solid black curves correspond to experimentally demonstrated amplification discussed in the text below.

these distributions, allowing for the copying fidelity to exceed  $\mathcal{F} = 5/6$  (universal cloning limit). However, the process is inherently probabilistic and cannot be directly employed for amplification: it produces two good copies with the probability  $P_A < 1/2$ .

Fortunately, it is also possible to find a classical deterministic strategy that uses *a priori* knowledge regarding

the state distribution to be cloned. It randomly swaps the original qubit with the mean state of the cloned distribution (the central state) [13]. The CBA can combine those two optimal strategies to amplify photonic qubits with a high probability  $P$ . The success rate of the CBA equals

$$P(\epsilon) = \epsilon + (1 - \epsilon)P_A \quad (5)$$

where  $\epsilon$  describes mixing the quantum ( $\epsilon = 0$ ) and the classical approach ( $\epsilon = 1$ ). For axially-symmetric cloning the success probability  $P_A$  equals

$$P_A = \frac{1}{6 \cos^2 \alpha_+} \left( \cos^2 \frac{\theta}{2} \cos^2 \alpha_+ + \sin^2 \frac{\theta}{2} \sin^2 \alpha_- \right) + \frac{1}{6 \cos^2 \alpha_-} \left( \sin^2 \frac{\theta}{2} \cos^2 \alpha_- + \cos^2 \frac{\theta}{2} \sin^2 \alpha_+ \right). \quad (6)$$

The result is optimal if  $\cos^2 \alpha_{\mp} \geq \sin^2 \alpha_{\pm}$ . The values of  $\alpha_{\pm}$  depend on the shape of the qubit distribution  $g(\rho)$  [22].  $P(\epsilon)$  can be arbitrarily close to one (deterministic regime), providing maximal gain  $G$  for  $\epsilon \simeq 1$  and  $\eta \ll 1$ ,  $G = 2P(\epsilon) \simeq 2$ . Note that  $P_A$  describes a general class of transformations including universal [12], phase-covariant [17] and mirror phase-covariant cloners [21].

Any spherical axisymmetric distribution function  $g(\rho) = g(\theta)$  can be expressed by the Legendre polynomials  $P_n(\cos \theta)$  as [31]:

$$g(\theta) = \frac{1}{4\pi} \sum_{n=0}^{\infty} (2n+1) a_n P_n(\cos \theta), \quad (7)$$

$$a_n = \int_0^{2\pi} \int_{-1}^1 g(\theta) P_n(\cos \theta) d \cos \theta d \phi. \quad (8)$$

Therefore, any results depending on  $g(\rho)$  can be expressed in terms of  $a_n$ . For a normalized qubit distribution ( $a_0 = 1$ ) one needs to know only  $a_1$  and  $a_2$  in order to fully characterize the corresponding optimal cloning transformation. For example, the values representing angles  $\alpha_{\pm}$  depend on a single parameter

$$\Gamma = \frac{6\sqrt{2}a_1(a_2 - 1)}{x_+ x_-}, \quad (9)$$

where  $x_{\pm} = 1 + 2a_2 \pm 3a_1$ . As long as  $|\Gamma| < 1$ , we can express the  $\alpha_{\pm}$  angles as

$$2\alpha_{\pm} = \arcsin \Omega \pm \arcsin \Gamma, \quad (10)$$

where

$$\Omega = \frac{2\sqrt{2}(1 + 2a_2)(1 - a_2)}{\sqrt{3x_+ x_- (3 + 4a_2^2 - 3a_1^2 - 4a_2)}}. \quad (11)$$

However, for  $|\Gamma| > 1$  there are two possibilities, i.e.,  $\alpha_+ = 0$  and  $\alpha_- = \frac{\pi}{2}$  or vice versa. The corresponding optimal cloning process in this case is the phase covariant cloning of Fiuřářek [19]. The case of  $a_1 = 0$  includes the equatorial phase covariant cloning for  $\theta = \pi/2$  and the mirror phase covariant cloning [21] ( $\alpha_+ = \alpha_-$ ). If  $a_1 = a_2 = 0$ , we obtain the universal cloning transformation [12]. The difference between the universal CBA

TABLE I. Comparison of the parameters of CBA using deterministic quantum cloning CBA<sub>DQC</sub> and CBA<sub>LO</sub>( $\epsilon = 0.5$ ) implemented within the framework of linear optics and using hybrid quantum-classical cloning. The data suggests that even for a large amount of classical cloning the CBA<sub>LO</sub>( $\epsilon = 0.5$ ) provides amplification (gain  $G > 1$ ) and produces signal that is better in quality than the best classical amplifier ( $F > 0.75$ ). The total transmissivity of the channel is  $\eta = \eta_A \eta_B = 0.01$ .

Amplifier	$\eta_A$	$\eta_B$	$G$	$P$	$\mathcal{F}$
CBA <sub>DQC</sub>	0.01	1.00	1.00	1.00	0.83
	0.50	0.02	1.98	1.00	0.83
	1.00	0.01	1.99	1.00	0.83
CBA <sub>LO</sub> ( $\epsilon = 0.5$ )	0.01	1.00	0.62	0.62	0.77
	0.50	0.02	1.23	0.62	0.77
	1.00	0.01	1.23	0.62	0.77

using deterministic quantum cloning and our hybrid approach (constrained by linear optics) is described quantitatively in Tab. I.

The average fidelity  $\mathcal{F}$  of the clones  $\rho'$  produced by the CBA equals the weighted average over the Poincaré sphere calculated using a measure  $d\omega = d\cos\theta d\phi$  (the Haar measure) suitable for the spherical geometry of the original qubits  $\rho = |\Psi\rangle\langle\Psi|$  multiplied by the distribution  $g(\rho)$ , i.e.,  $\mathcal{F} = \int d\omega g(\rho) \text{Tr}\{\rho\rho'\}$ , where  $\rho' = (1 - \epsilon)\rho_q + \epsilon\rho_c$ ,  $\rho_q$  is the best quantum copy, and  $\rho_c = (\sigma + \rho)/2$  is a state obtained by the classical strategy for  $\sigma$  being the best replacement for  $\rho$ . This expression is maximized if  $\sigma = \int d\omega \rho g(\rho)$ . For axially distributed input qubits  $|\Psi\rangle$  we obtain

$$\mathcal{F} = (1 - \varepsilon)\mathcal{F}_A + \frac{\varepsilon}{4}(3 + \langle\cos\theta\rangle^2) \quad (12)$$

where  $\varepsilon = \epsilon/P(\epsilon)$ ,  $\sigma = (\mathbb{1} + \langle\cos\theta\rangle\sigma_z)/2$ , and

$$\mathcal{F}_A = \frac{1}{8}[2(3 + \cos 2\alpha_+)\langle\cos^4 \frac{\theta}{2}\rangle + 2(3 + \cos 2\alpha_-)\langle\sin^4 \frac{\theta}{2}\rangle + (\sin^2 \alpha_+ + \sin^2 \alpha_- + 2\sqrt{2}\sin\Omega)\langle\sin^2 \theta\rangle], \quad (13)$$

is quantum cloning fidelity with  $\Omega = \alpha_+ + \alpha_-$  [22]. For the universal CBA one obtains  $\sin\alpha_{\pm} = 1/\sqrt{3}$  and  $\mathcal{F}_A = 5/6$  resulting in  $\mathcal{F}^u = (1 - \varepsilon)5/6 + 3\varepsilon/4$ .

To streamline our experiment we focused on axially-symmetric input qubit distributions with  $\langle\cos\theta\rangle = 0$  [see Fig. 4(a)] and  $\langle\cos\theta\rangle^2 = \langle\cos^2\theta\rangle$  [see Fig. 4(b)]. They encompass mirror phase-covariant, phase-covariant and universal cloners. If the mirror symmetry is slightly broken, the optimal QCM becomes a phase-covariant cloner [22] optimized for  $\langle\cos^2\theta\rangle = \langle\cos\theta\rangle^2$ , i.e.  $\cos\alpha_{\pm} = 1/\sqrt{2}$  and  $G(\epsilon) = 2(1 - \epsilon)/3 + 2\epsilon$ .

### III. COMPARISON WITH HERALDED AMPLIFIER

Both the HA and CBA are called “amplifiers” and are used to increase the probability of detecting a photon.

TABLE II. Comparison of the parameter of HA from Ref. [9] (it provides higher success probability than the scheme proposed in Ref. [3]) with the CBA<sub>LO</sub>( $\epsilon = 0.5$ ) implemented within the framework of linear optics and using hybrid quantum-classical cloning for  $\epsilon = 0.5$ . The parameter  $r = 0.294$  of the HA represents reflectivity of beamsplitters that is set so that gain of the amplifier will reach the one of the CBA for  $\eta_A = 0.5$ . If gain of both the amplifiers is the same, then CBA has superior success rate. However, CBA provides lower signal fidelity than the noiseless amplifier. The total transmissivity of the channel is  $\eta = \eta_A \eta_B = 0.01$ . The meaning of parameters  $\eta_A$  and  $\eta_B$  is explained in Fig. 2.

Amplifier	$\eta_A$	$\eta_B$	$G$	$P$	$\mathcal{F}$
CBA <sub>LO</sub> ( $\epsilon = 0.5$ )	0.01	1.00	0.62	0.62	0.77
	0.50	0.02	1.23	0.62	0.77
	1.00	0.01	1.23	0.62	0.77
HA( $r = 0.294$ )	0.01	1.00	1.58	0.09	1.00
	0.50	0.02	1.23	0.11	1.00
	1.00	0.01	1.00	0.14	1.00

Their principle of operation is very different. The HA increases this probability by rejecting cases when a photon is not likely to appear. The CBA does that by sending more photons. However, despite their differences the HA and the CBA have a lot in common. The term “amplifier” implies that there is some gain (in energy) and possibly some noise added. This is true for both cases, if we consider the number of photons received in a time window. For the CBA this window is just an arbitrary time interval. For the HA this time interval is the time over which the HA heralds the arriving photons (the remaining time can be used for some other purpose). It is natural to ask whether one of these amplifiers gives better results.

Here we will demonstrate that the two amplifiers perform complementary tasks. Depending on the amplification regime, one of the amplifiers becomes more useful than the other. We will assume that both the amplifiers are optimized for a uniform qubit distribution over the Bloch sphere. The results of our study are summarized in Tab. II.

#### A. Postamplification

When both the CBA and the HA are used at the end of the channel, the HA implements the following transformation [3, 6]

$$\rho'_{\text{in}} \rightarrow \rho_{\text{out}} = (1 - P)\rho_{\text{vac}} + P\rho'_{\text{out}}, \quad (14)$$

where the input state is the attenuated qubit  $\rho'_{\text{in}} = \eta\rho_{\text{in}} + (1 - \eta)\rho_{\text{vac}}$  and  $P$  is the success probability of the device. With probability  $P$  one can herald the state  $\rho'_{\text{out}} = \frac{1}{N}[(1 - \eta_B)\rho_{\text{vac}} + g^2\eta_B\rho]$ , where  $N = 1 - \eta_A + \eta_A g^2$ . The nominal gain of the HA is defined as  $G_{\text{nom}}^{(\text{HA})} = g^2/N$ . Nevertheless, the transmission gain of the HA has to in-

clude the probability of the successful operation of the device and is defined as

$$G_T^{(\text{HA})} = PG_{\text{nom}}^{(\text{HA})} \leq 1, \quad (15)$$

where the inequality can be saturated only for  $\eta_A = 1$ . However, if we are interested only in the cases when the arrival of the signal has been announced, the transmission gain reads

$$G_{T'}^{(\text{HA})} = G_{\text{nom}}^{(\text{HA})} > 1, \quad (16)$$

The experimentally observed success probability values are low, e.g.,  $P = 0.05$  for  $G_{\text{nom}}^{(\text{HA})} = 3.3 \pm 0.6$  in [6].

In comparison, if the input of the CBA is a damped photon in state  $\rho'_{\text{in}} = \eta_A \rho_{\text{in}} + (1 - \eta_A) \rho_{\text{vac}}$  and after the amplification process the photon is not damped, the transmission gain equals

$$G_T^{(\text{CBA})} = P \leq 1. \quad (17)$$

This means that the amplification gain defined as a ratio of probabilities of finding at least one photon at the output with and without amplification [see Eq. (2)] does not reveal the apparent increase in signal intensity caused by duplicating the signal. Using an alternative definition of transmission gain based on the ratio of the mean photon numbers with and without amplification would reveal that the signal intensity grows depending on  $P$ .

The fair comparison of the two amplifiers should be performed for gains  $G_T^{(\text{CBA})}$  and  $G_{T'}^{(\text{HA})}$ . Thus, in this scenario none of the amplifiers are useful for increasing the traditionally defined transmission rate (average transmission speed over the whole time of transmission). However, when the transmission gain for the HA is calculated only for the cases when the arrival of the photon is announced (average transmission speed over the time over which the signals were announced), the HA provides genuine amplification while CBA introduces losses and noise (for universal cloning qubit fidelity is  $\mathcal{F} \leq 5/6$ ). Placing the HA at the end of the line (where we have a mixture of vacuum and the initial signal) can noiselessly increase the probability of finding the heralded photon to one (i.e. infinite nominal gain), at the expense of lowering the probability of announcing the arriving signal (this is by design impossible with the CBA). The CBA becomes useful if there is some more damping ahead.

## B. Preamplification

For a fixed success rate  $P$ , the transmission gain of the CBA is twice as high as that of the HA, which can be seen if the output states of the two devices are compared for a low channel transmittance  $\eta_B \ll 1$ . The probability of finding at least one photon at the output of the CBA amplifier is  $P_{n>0}^{(\text{CBA})} = 2P\eta_B$ , whereas for the HA it reads  $P_{n>0}^{(\text{HA})} = P\eta_B$ . If none of the amplifiers is used  $P_{n>0}^{(0)} =$

$\eta_B$ . This results in  $G_T^{(\text{CBA})} \approx G = 2P > 1$ , if  $P > 1/2$ , for the CBA and  $G_T^{(\text{HA})} = P \leq 1$  (or  $G_{T'}^{(\text{HA})} = 1$ ) for the HA.

If we consider qubit subspace fidelity, then for the CBA it is equal  $\mathcal{F}$  and for the HA it equals 1. Thus, the HA performs better with regard to this figure of merit. Another important quantity for amplifiers is the output fidelity (as defined in Ref. [6]) defined for  $\rho_{\text{in}} = \rho$  and a single-mode output of the CBA as  $F_{\text{CBA}}^{(\text{output},1)} = \text{Tr}(\rho_{\text{out},1}\rho) = P\eta_B\mathcal{F}$ , where  $\rho_{\text{out},1}$  is the reduced single-copy density matrix of the first output (assuming that all the copies are the same) including  $\rho'$  and some vacuum. To perform a fair comparison we should sum contributions from all the output modes. In the limit  $\eta_B \ll 1$  the modes are independent because there is only a small chance of receiving both copies. If we now physically combine all output modes of the CBA we will obtain (for  $\eta \ll 1$  and  $1 \rightarrow 2$  cloning)

$$F_{\text{CBA}}^{(\text{output})} = N_{\text{copy}} \text{Tr}(\rho_{\text{out},1}\rho) = 2\eta_B P\mathcal{F}. \quad (18)$$

For a single-mode output of the HA the output fidelity becomes

$$F_{\text{HA}}^{(\text{output})} = \text{Tr}(\rho_{\text{out}}\rho) = \eta_B P. \quad (19)$$

This means that for a fixed success rate  $P$  and number of copies  $N_{\text{copy}} = 2$  the CBA is better than HA as long as  $2\mathcal{F} > 1$ , which is always true. If the fidelity  $\mathcal{F}$  of the CBA is optimized so that  $2P\mathcal{F} > 1$ , the CBA outperforms the HA when both amplify qubits at the beginning of the transmission line. Leaving the qubit unaltered is preferable to probabilistic heralding of its presence, even if the success probability of the HA equals 1.

## IV. THE EXPERIMENT

In our experiment we measure only  $\rho_{1,2}$  ( $\rho'$ ) and  $P$  (see Fig. 3), but these are enough to estimate  $G$  (for  $\eta \ll 1$ ) and  $\text{SNR}$ . For technical reasons we were not able to separate the unsuccessful quantum cloning events from other cases by means other than the postselection on the successful detection of  $\rho_{1,2}$ . Thus, our proof-of-principle experiment investigates channel-independent properties of a linear-optical CBA (as in the case of  $\eta \ll 1$ ).

### A. The source

Type I degenerate spontaneous parametric down-conversion (1 cm long  $\text{LiIO}_3$  crystal) generates pairs of photons used as input states. The crystal is pumped by a 413 nm continuous wave  $\text{Kr}^+$  laser (200 mW). Half-wave (HWP) and quarter wave plates (QWP) encode the qubits in a photonic polarization. The signal photon ("in") is further amplified, the idler ("anc") becomes an ancillary photon whose state depends on the type of cloning used in the CBA. Figure 5 shows the implementation setup of the CBA.

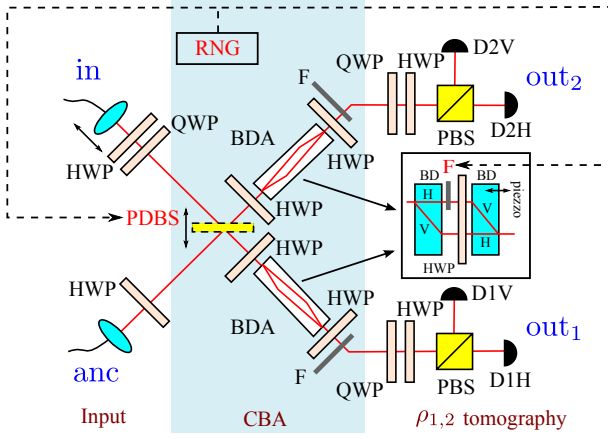


FIG. 5. (Color online) Implementation of the cloning-based quantum amplifier (CBA). A random number generator RNG provides a number  $r \in [0, 1]$  and switches the device between its two regimes of work: optimal quantum cloning (if  $r \leq 1 - \epsilon$ ) and the mixing of input qubit  $\rho$  with the central state  $\sigma$  (if  $r > 1 - \epsilon$ ). The latter regime requires removing the PDBS and filters F from BDAs. PDBS, polarization dependent beam splitter; BD, beam displacer; BS, beam splitter; HWP (QWP), half (quarter) wave plate; F, neutral density filter. After the signal  $\rho$  and ancillary photons are prepared (by means of HWPs and a QWP) they interact on a PDBS. Next, if the photons exit at separate ports, a specific polarization component (set by HWPs) of both photons is attenuated in the respective BDAs (another pair of HWPs restores the original polarization). Just before exiting the CBA the intensity in both output ports is balanced by a pair of neutral density filters F. Finally, a polarization analysis is performed.

### B. Optimal quantum cloning

The first strategy is quantum-based ( $\epsilon = 0$ ). The device functions as a phase-covariant and mirror phase-covariant cloner [23]. The optimal cloning transformation can be now written in the form of a unitary transformation

$$|HHH\rangle \rightarrow \cos \alpha_+ |HHV\rangle + \sin \alpha_+ |\psi_+\rangle |H\rangle, \quad (20a)$$

$$|VHH\rangle \rightarrow \cos \alpha_- |VVH\rangle + \sin \alpha_- |\psi_+\rangle |V\rangle, \quad (20b)$$

where  $|\psi_+\rangle = (|HV\rangle + |VH\rangle) / \sqrt{2}$ . The first mode is the signal mode, the last two correspond to ancillary modes. After the transformation the clones are encoded in the last two modes and the third mode is removed. The unitary transformation could be implemented in a deterministic way in a properly tailored system. However, being limited by linear optics, in our experiment we perform an equivalent stochastic operation consisting of two operations involving only two-photon interactions

$$|HH\rangle_{\text{in,anc}} \rightarrow \cos \alpha_+ |HH\rangle_{1,2}, \quad (21a)$$

$$|VH\rangle_{\text{in,anc}} \rightarrow \sin \alpha_- |\psi_+\rangle_{1,2}, \quad (21b)$$

and

$$|HV\rangle_{\text{in,anc}} \rightarrow \sin \alpha_+ |\psi_+\rangle_{1,2}, \quad (22a)$$

$$|VV\rangle_{\text{in,anc}} \rightarrow \cos \alpha_- |VV\rangle_{1,2}. \quad (22b)$$

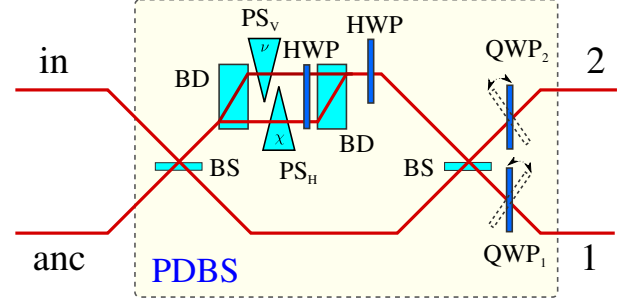


FIG. 6. (Color online) Implementation of polarization dependent beam splitter PDBS: BD, beam displacer; BS, symmetric beam splitter; HWP (QWP<sub>1,2</sub>), half (quarter) wave plate; PS<sub>H(V)</sub>, phase shifter. By manipulating the phase shifts  $\nu$  and  $\chi$  of H and V polarization components respectively, the interferometer acts as a PDBS with variable reflection and transmittance for each of the H and V polarizations. To remove the phase difference  $\nu - \chi$  between the phases of V and H polarization component of both output modes, we use QWP<sub>1</sub> and QWP<sub>2</sub> (or Pockels cells) set to shift phases of V-polarized photons by  $\chi - \nu$ . It can be verified that the setup output may be expressed in terms of annihilation operators as  $a_{2,s} = \sqrt{\eta_s} a_{\text{anc},s} - \sqrt{1 - \eta_s} a_{\text{in},s}$ ,  $a_{1,s} = \sqrt{\eta_s} a_{\text{in},s} + \sqrt{1 - \eta_s} a_{\text{anc},s}$ , where  $\eta_s = \cos^2 \chi, \cos^2 \nu$  for  $s = H, V$ , respectively. If there is no phase shift, the PDBS acts as if it was removed.

The transformations are probabilistic and they work with the success rate  $P_A$ . The ancillary photon is polarized either horizontally or vertically. The signal and ancillary photons interfere on a polarization dependent beam splitter (PDBS).

Repeated scanning of the Hong-Ou-Mandel dip ensures interferometric stability. This is achieved by shifting the PDBS mounted on a motorized translation stage and fixing it in the optimal position. The PDBS implemented as a Mach Zehnder interferometer including conventional beam splitters (BS), phase shifters (PS), a wave plate and beam dividers (BD) is shown in Fig. 6. Overall PDBS transmittivities obtained experimentally equal  $\eta_H = 76\%$  and  $\eta_V = 18\%$  for horizontal and vertical polarizations, respectively. To maximize the output state fidelity polarization dependent filtration is applied in both output ports of the PDBS by two blocks (see BDA blocks in Fig. 5) consisting of two BDs splitting and subsequently merging horizontal and vertical polarizations, and a neutral density filter placed between them introducing polarization dependent losses. Filtering corrects beam splitter imperfections at the expense of success probability  $P_A$ . It also allows us to optimize the setup for various  $\alpha_{\pm}$ . If no filtering is applied, the setup (consisting only of the PDBS) approximates a transformation corresponding to phase-covariant cloning with  $P_A \approx 1/3$ , i.e.,

$$|HH\rangle_{\text{in,anc}} \rightarrow |HH\rangle_{1,2}, \quad (23a)$$

$$|VH\rangle_{\text{in,anc}} \rightarrow |\psi_+\rangle_{1,2}, \quad (23b)$$

and

$$|HV\rangle_{\text{in,anc}} \rightarrow |\psi_+\rangle_{1,2}, \quad (24a)$$

$$|VV\rangle_{\text{in,anc}} \rightarrow |VV\rangle_{1,2}. \quad (24b)$$

With probability  $1 - P_A$  the two photons bunch in one output port, hence the cloning operation fails. It is apparent that to introduce the scaling factors used for an arbitrary axially symmetric cloning we have to attenuate the H (V) polarization in both output modes by the same amount, depending on the state of the ancillary photon. For more technical details on implementing multifunctional quantum cloning see Refs. [23, 32].

### C. Optimal classical cloning

The second strategy constitutes classical copying. It requires removing the PDBS and setting the ancillary state as the central state  $\sigma$  of the signal state distribution. The signal and ancillary photons propagate without interference (all filters are removed). The signal and ancillary modes are swapped with probability  $1/2$ . Our setup permits to deterministically prepare an arbitrary ancillary and signal state with almost perfect fidelity with respect to the target state.

### D. Hybrid cloning

A random number generator (RNG) switches the device between two regimes of work, permitting two different strategies (quantified by  $\epsilon$ ) described below. The RNG provides a random number  $r \in [0, 1]$  given by a uniform distribution. If this number satisfies  $r \leq 1 - \epsilon$ , the quantum strategy is implemented, else ( $r > 1 - \epsilon$ ) the classical strategy is applied.

### E. Data analysis

A complete two-photon polarization tomography is performed in both strategies [33]. To do that we project the states at the two output ports  $\text{out}_{1(2)}$  to horizontal, vertical, diagonal and anti-diagonal linear polarizations and right- and left-hand circular polarizations. Time-bin encoding can be used to deterministically combine the two output modes into a single mode suitable for transmission through a single optical fiber. Here the modes are separated for practical reasons. Photons are detected in both modes by the single photon counting modules (detectors), and the numbers of coincidences per 5 s intervals are registered for all relevant two-mode polarizations. Typically, we accumulate about 100 000 coincidences for each output state. The maximum likelihood method is used to reconstruct the photonic polarization density matrices [34]. The matrices are used to derive the experimental values of  $SNR$  for a given gain  $G = 2P$ .

To determine  $P$  we compare the calibration coincidence rate with that observed during the measurements. The former is measured in the setup with the PDBS shifted out of its position so that the reflection is no longer coupled to the detectors. All filters are retracted. This is how we distinguish between technological losses (caused by the 50% single photon detection efficiency, imperfect fiber coupling, and back-reflection) and the fundamental success probability of the procedure [23].

Figure 7 depicts the  $SNR$  ratio and gain  $G$  measured for the CBA with the mixing parameter  $\epsilon = 1/2$  as a function of the input qubit distribution on the Poincaré sphere, parametrized by  $\langle \cos^2 \theta \rangle$ , with  $\langle \cos \theta \rangle = 0$  (mirror phase-covariant distributions). The fidelity of the universal CBA  $\mathcal{F}_{\text{exp}}^u = 0.758 \pm 0.018$  is, because of losses  $\varepsilon_{\text{th}} < \varepsilon_{\text{ex}}$ , smaller than its theoretical value  $\mathcal{F}_{\text{th}}^u \approx 0.77$ . These values constitute the lowest fidelities for the CBA in this regime. However, both of these values are above the quantum amplification threshold for universal copying. The fidelities of the phase-covariant CBA for equatorial qubits  $\mathcal{F}_{\text{exp}}^{\text{pc}} = 0.768 \pm 0.004$  and of the classical (polar) CBA  $\mathcal{F}_{\text{exp}}^c = 0.773 \pm 0.012$  follow the trend of their theoretical values:  $\mathcal{F}_{\text{th}}^{\text{pc}} = 0.78$ ,  $\mathcal{F}_{\text{th}}^c = 0.79$ . The success rates for these three CBAs for  $\epsilon = 1/2$  equal:  $P_{\text{th}}^u = 5/8$  ( $P_{\text{exp}}^u = 0.598 \pm 0.018$ ),  $P_{\text{th}}^{\text{pc}} = 2/3$  ( $P_{\text{exp}}^{\text{pc}} = 0.624 \pm 0.005$ ),  $P_{\text{th}}^c = 7/12$  ( $P_{\text{exp}}^c = 0.553 \pm 0.014$ ). Experimental results place below the theoretical curves for the ideal setup components (solid) due to the imperfections of the PDBS. The setup was optimized for  $SNR$  which lowered the value of gain  $G$  by approx. 0.2 dB. Note that the PDBS-related imperfections are not included in the technological losses defined above and, consequently, have an influence on the calculated success probabilities. We also examined the performance of the device in Fig. 5 operating in the classical ( $\epsilon = 1$ ), quantum ( $\epsilon = 0$ ), and intermediate ( $0 < \epsilon < 1$ ) regimes. The  $SNR$  was measured as a function of  $G$ , parametrized by  $\epsilon$ . As shown in Fig. 4, two qubit distributions with  $\langle \cos^2 \theta \rangle = 1/3$  and  $\langle \cos^2 \theta \rangle = 0$ , both for  $\langle \cos \theta \rangle = 0$ , were given as input. The shaded areas of  $G > 0$  dB and  $SNR > 0$  dB show where the device functions as a universal and phase-covariant CBA.

As shown in Fig. 1, there are two distinct regimes in which the cloning machine can operate. The first one, described in detail in the paper, is the mirror phase-covariant regime, the other is the phase-covariant regime. The difference between these two regimes is that in the later case we have more a priori knowledge about the hemisphere from which the amplified qubits are selected. In the extreme case of the poles, cloning can be done in a perfect way since we know everything about the copied state. This is confirmed experimentally and the results are shown in Fig. 9. This figure shows that with the increase of the *a priori* knowledge about the states being copied we can improve the parameters of the amplifier in comparison with the universal case where the qubits to be amplified are evenly distributed over the Bloch sphere.

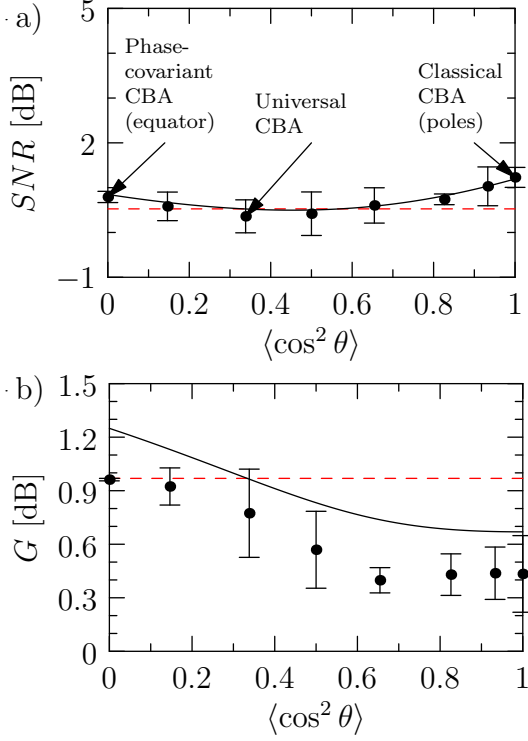


FIG. 7. (Color online) Signal-to-noise ratio  $SNR$  and amplification gain  $G$  measured for the cloning-based amplifier (CBA) with the mixing parameter  $\epsilon = 1/2$  as a function of the input qubit distribution on the Poincaré sphere, parametrized by  $\langle \cos^2 \theta \rangle$  with  $\langle \cos \theta \rangle = 0$ , i.e., mirror phase-covariant regime (see Fig. 9 for  $\langle \cos^2 \theta \rangle = \langle \cos \theta \rangle^2$  regime). Dashed lines indicate the value of fidelity and gain for the universal CBA. The details are given in the main text.

## V. CONCLUSIONS

This paper presents a high-fidelity near-deterministic genuine qubit amplifier (see Figs. 7 and 8). In contrast to heralded qubit amplifiers, our device produces pairs of photons with  $P > \frac{1}{2}$ . In this sense it increases the photon rate and achieves genuine amplification. Because this effect is obtained at the expense of added noise we analyzed the signal to noise ratio vs. the gain trade-off. The experimental data fit the theoretical prediction, confirming amplifier functionality. The CBA does not work properly if the cloning procedure fails by sending both photons to  $out_1$  or  $out_2$  (see Fig. 5). In our experiment we exclude such events by coincidence detection but a full-field implementation will require other solutions (see, e.g., [35] and references therein).

We compare the CBA working in a quantum regime ( $\epsilon = 0$ ) to the stimulated emission process used for cloning. Since the available nonlinearities in media are small, the efficiency of phase-covariant cloning is very low: approx. 0.01 [36]. The efficiency of the CBA equals 0.29, although the theoretical limit equals  $\frac{1}{3}$ . However, this limitation is platform dependent and in other, more

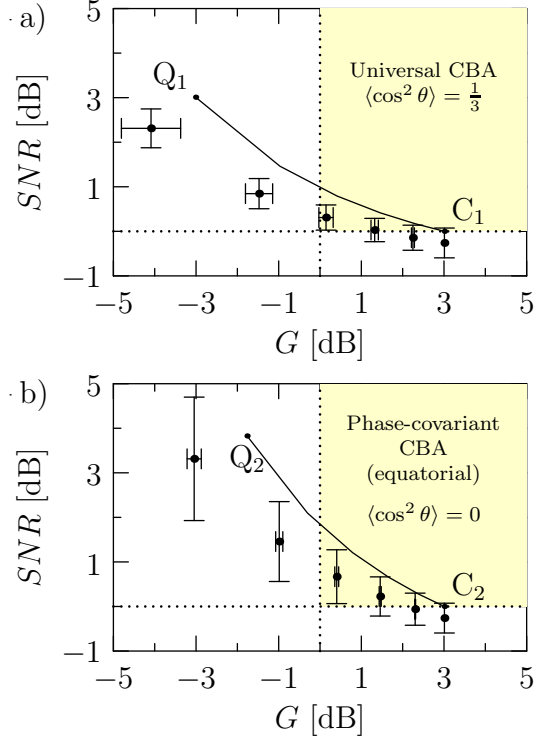


FIG. 8. (Color online)  $SNR$  as a function of gain  $G$  measured by the device from Fig. 5 for input qubit distribution  $\langle \cos^2 \theta \rangle = 1/3$  (left) and  $\langle \cos^2 \theta \rangle = 0$  (right) for  $\langle \cos \theta \rangle = 0$ . Solid curves show theoretical predictions for the ideal setup components, assuming the device operates on a scale from purely quantum  $Q_1 = (-3.01, 3.01)$  and  $Q_2 = (-1.76, 3.83)$  ( $\epsilon = 0$ ) to classical  $C_{1(2)} = (3.01, 0)$  ( $\epsilon = 1$ ) regime. The marked areas of  $G > 0$  dB and  $SNR > 0$  dB highlight the part of the regime where the device works as the universal and phase-covariant CBA.

advanced implementations it could reach 1.

Stimulated emission based amplification strongly depends on the power of the amplified signal and is inefficient if the average number of photons in the signal is too small. In this regime the CBA is potentially very useful, for the analysis of quantum channels with phase-independent damping as it extends the range of quantum communication. In particular, we have demonstrated (see Fig. 9) that our implementation of CBA can yield values of  $G$  and  $SNR$  that are large enough to increase product state capacity of the transmission channel described by Eq. (1).

## ACKNOWLEDGMENTS

K. B. gratefully acknowledges the support from the Operational Program Research and Development for Innovations – European Regional Development Fund (project CZ.1.05/2.1.00/03.0058 and the Operational Program Education for Competitiveness - European So-

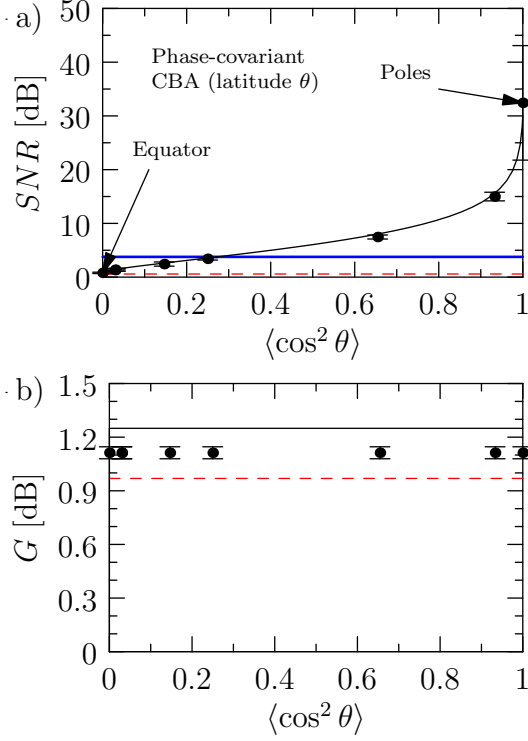


FIG. 9. (Color online) Signal-to-noise ratio  $SNR$  and amplification gain  $G$  measured for the cloning-based amplifier (CBA) with mixing parameter  $\epsilon = 1/2$  as a function of the input qubit distribution on the Poincaré sphere, parametrized by  $\langle \cos^2 \theta \rangle$  with  $\langle \cos^2 \theta \rangle = \langle \cos \theta \rangle^2$ , i.e., phase-covariant regime. Red dashed lines indicate the value of fidelity and gain for the universal CBA. Green dotted line indicates the  $SNR$  above which the CBA provides improvement in product state capacity [see Eq. (1)] for  $\eta \ll 1$ .

cial Fund (project CZ.1.07/2.3.00/20.0017 of the Ministry of Education, Youth and Sports of the Czech Republic. K. L. acknowledges support by the Czech Science Foundation (Grant no. 13-31000P). This work was also supported by the Polish National Science Centre under grant DEC-2011/03/B/ST2/01903. M. S. was supported by the EU 7FP Marie Curie Career Integration Grant No. 322150 “QCAT”, NCN grant No. 2012/04/M/ST2/00789, FNP Homing Plus project No. HOMING PLUS/2012-5/12 and MNiSW co-financed international project No. 2586/7.PR/2012/2.

- 
- [1] H.-J. Briegel, W. Dür, J.-I. Cirac and P. Zoller, *Phys. Rev. Lett.* **81**, 5932 (1998).
  - [2] A. Carlini, M. Sasaki, *Phys. Rev. A* **68**, 042327 (2003).
  - [3] N. Gisin, S. Pironio and N. Sangouard, *Phys. Rev. Lett.* **105**, 070501 (2010).
  - [4] M. Stobińska, P. Sekatski, A. Buraczewski, N. Gisin, and G. Leuchs, *Phys. Rev. A* **84**, 034104 (2011); M. Stobińska, F. Töppel, P. Sekatski, A. Buraczewski, M. Żukowski, M. V. Chekhova, G. Leuchs, and N. Gisin, *Phys. Rev. A* **86**, 063823 (2012); A. Buraczewski and M. Stobińska, *Comp. Phys. Commun.* **183**, 2245 (2012); M. Stobińska, F. Töppel, P. Sekatski, and A. Buraczewski, *Phys. Rev. A* **89**, 022119 (2014).
  - [5] A. I. Lvovsky, *Nat. Phys.* **9**, 5 (2013).
  - [6] G.Y. Xiang, T.C. Ralph, A.P. Lund, N. Walk, and G.J. Pryde, *Nat. Photon.* **4**, 316 (2010); S. Kocsis, G.Y. Xiang, T.C. Ralph, and G.J. Pryde, *Nat. Phys.* **9**, 23 (2013).
  - [7] D. Pitkanen, X. Ma, R. Wickert, P. van Loock, and N. Lütkenhaus, *Phys. Rev. A* **84**, 022325 (2011).
  - [8] M. Curty and T. Moroder, *Phys. Rev. A* **84**, 010304(R) (2011).
  - [9] E. Meyer-Scott, M. Bula, K. Bartkiewicz, A. Černoč, J. Soubusta, T. Jennewein, and K. Lemr, *Phys. Rev. A* **88**, 012327 (2013).
  - [10] K. Bartkiewicz, A. Černoč, K. Lemr, *Phys. Rev. A* **88**, 062304 (2013).
  - [11] W.K. Wootters and W.H. Zurek, *Nature (London)* **299**, 802 (1982); D. Dieks, *Phys. Lett.* **92A**, 271 (1982).
  - [12] V. Buzek and M. Hillery, *Phys. Rev. A* **54**, 1844 (1996).
  - [13] V. Scarani, S. Iblisdir, N. Gisin, and A. Acin, *Rev. Mod. Phys.* **77**, 1225 (2005); N.J. Cerf and J. Fiurášek, in *Progress in Optics* **49**, edited by E. Wolf (Elsevier, Amsterdam, 2006), pp. 455–545.
  - [14] L. Gyongyosi and S. Imre, *WSEAS Trans. Commun.* **9**, 165 (2010); C. H. Bennett and G. Brassard, in *Proceedings of the IEEE International Conference on Computers, Systems, and Signal Processing*, Bangalore, India, 1984 (IEEE, New York, 1984), p. 175; C. A. Fuchs, N. Gisin, R. B. Griffiths, C.-S. Niu, and A. Peres, *Phys. Rev. A* **56**, 1163 (1997); D. Bruss, *Phys. Rev. Lett.* **81**, 3018 (1998); H. Bechmann-Pasquinucci and N. Gisin, *Phys. Rev. A*

- 59**, 4238 (1999).
- [15] K. Bartkiewicz, K. Lemr, A. Černocho, J. Soubusta, and A. Miranowicz, Phys. Rev. Lett. **110**, 173601 (2013).
  - [16] N. Cerf, Phys. Rev. Lett. **84**, 4497 (2000).
  - [17] D. Bruss, M. Cinchetti, G. M. D'Ariano, and C. Macchiavello, Phys. Rev. A **62**, 012302 (2000).
  - [18] N. Gisin and S. Massar, Phys. Rev. Lett. **79**, 2153 (1997).
  - [19] J. Fiurasek, Phys. Rev. A **67**, 052314 (2003).
  - [20] J. Z. Hu, Z. W. Yu, and X. B. Wang, Euro. Phys. J. D **51**, 381 (2009).
  - [21] K. Bartkiewicz, A. Miranowicz, and Ş. K. Özdemir, Phys. Rev. A **80**, 032306 (2009).
  - [22] K. Bartkiewicz, A. Miranowicz, Phys. Rev. A **82**, 042330 (2010).
  - [23] K. Lemr, K. Bartkiewicz, A. Černocho, J. Soubusta, and A. Miranowicz, Phys. Rev. A **85**, 050307(R) (2012).
  - [24] R. A. Fisher, Proc. Roy. Soc. A **217**, 295 (1953).
  - [25] C. Brosseau, Appl. Opt. **34**, 4788 (1995).
  - [26] L. Henyey and J. Greenstein, Astrophys. J. **93**, 70 (1941).
  - [27] K. V. Mardia and P. E. Jupp, Directional statistics, vol. **494** (Wiley, 2009).
  - [28] M. Wilde, *Quantum Information Theory* (Cambridge University Press, Cambridge, 2013).
  - [29] F. De Martini and F. Sciarrino, Rev. Mod. Phys. **84**, 1765 (2012).
  - [30] F. Sciarrino and F. De Martini Phys. Rev. A **76**, 012330 (2007).
  - [31] W. Kaplan, *Advanced Calculus* (Addison-Wesley, Reading, MA, 1992).
  - [32] K. Bartkiewicz, A. Miranowicz, Phys. Scr. **T147**, 014003 (2012).
  - [33] E. Halenková, A. Černocho, K. Lemr, J. Soubusta, and S. Drusová, Appl. Opt. **51** (4), 474–478 (2012).
  - [34] M. Ježek, J. Fiurášek, and Z. Hradil, Phys. Rev. A **68**, 012305 (2003).
  - [35] M. J. Everitt, T. P. Spiller, G. J. Milburn, R. D. Wilson, A. M. Zagorskin, arXiv:1212.4795v2.
  - [36] C. Simon, G. Weihs, and A. Zeilinger, Phys. Rev. Lett. **84**, 2993 (2000).